


Gut Microbiota Metabolite, Trimethylamine N-Oxide, Aggravates Cognitive Impairment in Cerebral Ischemia–Reperfusion Injury

Wei Li^{1,2}, Jidian Jiang³, Jin Zhou³, Pengfei Li², Xiaoxia Duan² 

¹Department of Anesthesiology, Hejiang People's Hospital, Luzhou, Sichuan, 646200, People's Republic of China; ²Department of Anesthesiology, The Affiliated Hospital, Southwest Medical University, Luzhou, Sichuan, 646000, People's Republic of China; ³Department of Anesthesiology, Suining First People's Hospital, Suining, Sichuan, 629000, People's Republic of China

Correspondence: Xiaoxia Duan, Department of Anesthesiology, The Affiliated Hospital, Southwest Medical University, Luzhou, Sichuan, 646000, People's Republic of China, Email duanxiaoxia@swmu.edu.cn

Purpose: Cerebral ischemia–reperfusion injury (CIRI) causes neuronal inflammation, oxidative stress, and cognitive impairment. We hypothesized that gut microbiota dysbiosis exacerbates post-ischemic cognitive deficits, with trimethylamine N-oxide (TMAO) acting as a potential mediator.

Methods: In the primary experiment, mice received an antibiotic cocktail for 28 days to induce gut dysbiosis prior to bilateral common carotid artery occlusion (BCCAO), a model of CIRI (n = 12 per group). Gut microbial composition was analyzed using 16S rRNA sequencing, and cognitive function was assessed with the Morris water maze. Functional enrichment analyses (Kyoto Encyclopedia of Genes and Genomes and Clusters of Orthologous Groups) and microbiota–metabolite database mapping were used to identify candidate metabolites. In a separate validation cohort (n = 6 per group), TMAO (6.5 mg/day) was administered intraperitoneally for 7 days before BCCAO.

Results: Antibiotic treatment markedly altered microbial diversity and composition, characterized by an expansion of Proteobacteria and a reduction in Lactobacillus. Bioinformatic analyses identified TMAO, a metabolite associated with Proteobacteria/Enterobacteria, as a potential mediator. Mice with antibiotic-induced dysbiosis subjected to CIRI exhibited impaired spatial memory, as indicated by fewer platform crossings and reduced time spent in the target quadrant. Similarly, TMAO pretreatment reproduced these cognitive deficits in BCCAO mice.

Conclusion: Antibiotic-induced gut dysbiosis appears to exacerbate CIRI-related cognitive impairment, at least in part through elevated TMAO levels. These findings highlight a potential microbiota–metabolite axis as a target for therapeutic intervention.

Keywords: gut microbiota, gut microbiome, cerebral ischemia-reperfusion injury, cognitive function, trimethylamine N-oxide

Introduction

When blood flow is restored to an ischemic brain region, a cascade of events known as cerebral ischemia–reperfusion injury (CIRI) is triggered. These reactions are common in patients with stroke and may lead to brain injury, edema, hemorrhage, and neuronal death.^{1,2} CIRI can cause varying degrees of cognitive impairment and motor dysfunction, such as hemiparesis and muscle weakness, thereby increasing disability and mortality.^{3–5} The reported incidence of CIRI-induced cognitive impairment is 40–70%.¹ Therefore, clarifying the mechanisms underlying CIRI-induced cognitive impairment is important.

The gut microbiota is an essential component of physiological homeostasis.⁶ The health of the human intestinal microbiota depends on a balanced gut microbiota environment,⁷ which is also crucial for neurological development and mitigating brain inflammation.⁸ Gut microbiota dysbiosis can induce sustained inflammation, nutrient and vitamin deficiencies, neurotransmitter imbalances, accumulation of toxic metabolites, and disruption of the gut–brain axis, all of which may contribute to cognitive dysfunction.⁹ Exacerbation of ischemia-induced brain injury and functional abnormalities has also been shown after transplantation of gut microbiota from patients with stroke or from experimental models into germ-free animals or into mice

receiving antibiotic treatment.^{10,11} Together, these findings suggest that gut microbiota dysbiosis may worsen CIRI-induced cognitive impairment, potentially through neuroinflammatory mechanisms.

Gut microbiota dysbiosis impairs cognitive function¹² by allowing inflammatory and neurotoxic substances to enter the central nervous system.¹³ Proinflammatory cytokines bind to specific receptors and transporters on endothelial cells of the blood–brain barrier, facilitating their entry into the central nervous system and triggering neuroinflammation.¹⁴ Metabolites such as bile acids, 5-hydroxyindoleacetic acid, and trimethylamine-N-oxide (TMAO) are markedly elevated in the body during gut microbial dysbiosis.^{15,16} TMAO can cross the blood–brain barrier and promote inflammation and oxidative stress, exacerbate microglial activation, and initiate neuroinflammatory responses, ultimately contributing to cognitive impairment–related disorders in older adults, including post-stroke cognitive impairment, Alzheimer’s disease (AD), and postoperative cognitive dysfunction.^{17,18} It is important to note that the gut–brain axis involves multiple interconnected pathways, including neural, endocrine, and immune routes, and TMAO is only one of many microbiota-derived metabolites that may influence brain function. However, the specific metabolic products through which gut microbiota dysbiosis exacerbates cognitive impairment after CIRI require further investigation.

In the present study, a cocktail of ciprofloxacin, ampicillin, streptomycin, and clindamycin was orally administered to induce gut microbiota dysbiosis in mice. These antibiotics were chosen to achieve broad-spectrum depletion of both Gram-negative and Gram-positive bacteria, a common strategy to induce gut dysbiosis.¹⁹ High-throughput sequencing of 16S ribosomal RNA (rRNA) was subsequently performed to characterize microbial alterations. Potential mechanisms by which gut microbiota dysbiosis exacerbates CIRI-induced cognitive deficits were explored using functional enrichment analyses, including the Kyoto Encyclopedia of Genes and Genomes (KEGG) and Clusters of Orthologous Groups (COG), together with database mining focused on microbial metabolism. Finally, a rodent model with elevated TMAO levels was established to validate its role in aggravating CIRI-induced cognitive impairment.

Materials and Methods

Experimental Animals and Design

Seventy-two healthy male C57BL/6J mice (6–8 weeks old, 20–25 g) were obtained from Beijing HFK Biotechnology Co., Ltd. (Beijing, China). The mice were housed under controlled conditions at 23–25 °C with a 12-h light/dark cycle and provided with unlimited access to feed and water. To assess the impact of gut microbiota dysbiosis on CIRI-induced cognitive impairment, mice were randomly divided into four groups: control (CON), antibiotic treatment (ABX), CIRI, and ABX + CIRI (n = 12 per group). The CON group remained undisturbed throughout the experiment with continuous access to feed and water. Mice in the ABX group received a mixed antibiotic solution in their drinking water for 28 days, which included ciprofloxacin, ampicillin, streptomycin, and clindamycin. The final concentration of each antibiotic in the drinking water was approximately 0.54 mg/mL. The antibiotic-containing water was freshly prepared every 3 days during the 28-day treatment period to minimize degradation. For the CIRI model, mice were anesthetized with an abdominal injection of 1% sodium pentobarbital (50 mg/kg) before undergoing bilateral common carotid artery occlusion (BCCAO) for 60 min. The neck arteries were exposed and temporarily occluded using microvascular clips. After recovery from anesthesia, the incision was sutured and covered with a sterile dressing, and the mice were returned to the barrier facility. The CON and ABX groups underwent neck artery exposure without occlusion. Mice in the ABX + CIRI group were administered the antibiotic solution for 28 days before BCCAO induction. Eight fresh fecal samples were randomly collected from each mouse and stored at –80 °C for subsequent analysis ([Supplementary Figure S1A](#)). Behavioral assessments and data analysis were performed by investigators blinded to group allocation.

To investigate whether elevated TMAO levels exacerbate CIRI-induced cognitive deficits, mice were randomly assigned to four groups (n = 6 per group): control (CON), TMAO, CIRI, and TMAO + CIRI. The CON group had free access to feed and water throughout the study. Based on previous studies, TMAO (6.5 mg/day) can effectively affect systemic and neurological processes in mice without substantial toxicity.^{20,21} Mice in the TMAO group received intraperitoneal injections of TMAO (6.5 mg/day) for 7 days, following a 25-day acclimatization period. The CIRI group underwent BCCAO modeling. Prior to BCCAO modeling, mice in the TMAO + CIRI group were also administered TMAO injections for 7 days

([Supplementary Figure S1B](#)). At the end of the experiment, mice were euthanized under anesthesia with 1% pentobarbital sodium, and serum and tissues were collected for subsequent experiments.

16S rRNA Gene Sequencing

After 28 days of drinking the mixed antibiotic solution, fresh fecal samples from eight mice in each group were randomly collected and stored at -80°C for future use. Fecal bacterial genomic DNA was extracted using the QIAamp PowerFecal Pro DNA Kit (Qiagen, USA). The integrity of the extracted DNA was evaluated using 1% agarose gel electrophoresis. The V3–V4 region of the 16S rRNA gene was amplified with specific primers (338F, ACTCCTACGGGAGGCAGCAG; 806R, GGACTACHVGGGTWTCTAAT) using TransStart Fastpfu DNA Polymerase (TransGen, China) in a 20- μL polymerase chain reaction (PCR) volume on a GeneAmp 9700 PCR System (ABI, USA). The resulting PCR products were purified using the AxyPrep DNA Gel Recovery Kit (Axygen, USA) and quantified using the QuantiFluor-ST Blue Fluorescence Quantification System (Promega, USA). Sequencing was conducted by Shanghai Majorbio Bio-pharm Technology Co., Ltd. (Shanghai, China) using the Illumina MiSeq platform. The quality-controlled data were clustered into operational taxonomic units (OTUs) based on an algorithm from the Ribosomal Database Project, with high-quality reads grouped at 97% nucleotide similarity. The relative abundance of microbial communities at the phylum, class, order, family, and genus levels for each sample was annotated based on OTUs using the Silva database (Release 138, <http://www.arb-silva.de>). Alpha diversity was assessed using the Chao1 richness index, Simpson index, and Shannon diversity index.

Principal coordinate analysis (PCoA), based on a distance matrix, was used to describe the relationships between samples and assess the β -diversity of sample community composition. Linear discriminant analysis effect size (LEfSe) was used to identify differences in microbial community composition between the two groups from the class to family levels. PICRUST (Phylogenetic Investigation of Communities by Reconstruction of Unobserved States) was used to normalize the OTU abundance table and infer corresponding COG and KEGG Ortholog (KO) profiles, followed by quantification of their respective abundances. COG data were used to derive functional abundance profiles from the eggNOG database, whereas KEGG information was used to obtain pathway-level abundance tables. The gutMGene database (<http://bio-annotation.cn/gutmgene>) was used to explore correlations between differentially abundant gut microbes, their metabolites, and host genes.

Quantitative Polymerase Chain Reaction (qPCR)

Quantitative PCR (qPCR) was performed using the ViiA 7 Real-Time PCR System (Applied Biosystems, USA) to validate the microbial sequencing results. Each amplification reaction contained 10 μL of SYBR qPCR Premix (Shaoxing Tongchuang Medical Equipment Co., Ltd.), 8 μL of primers (0.2–0.6 $\mu\text{mol/L}$), and 2 μL of template DNA or water as a negative control, for a total volume of 20 μL . All reactions were conducted in triplicate, ensuring a cycle threshold (Ct) difference of less than 0.5 among replicates. The thermal cycling protocol included an initial denaturation step at 95°C for 3 min, followed by 40 cycles of denaturation at 95°C for 15s, annealing for 30s, and extension at 60°C with fluorescence signal acquisition. Standard curves were constructed using plasmid templates of known concentrations, which were subsequently amplified with primers specific to the target microbes. Relative abundance was calculated using the $2^{-\Delta\Delta\text{Ct}}$ method.

Morris Water Maze

The Morris water maze (MWM) test was used to assess the spatial memory and learning abilities of rodents. A cylindrical pool was filled with water and colored white to enhance visibility. The pool was divided into four quadrants, each marked with distinct geometric cues for orientation. In the center of the target quadrant (quadrant 4), a submerged platform was placed 0.02 m below the water surface. The experiment was conducted over 5 days, consisting of acquisition trials that measured learning capacity through metrics such as swim distance and the time taken to locate the platform. On the final day, a probe trial was conducted to evaluate spatial memory, during which the number of platform crossings and the duration spent in the target quadrant were recorded. Behavioral testing was performed by investigators blinded to group allocation.

Enzyme-Linked Immunosorbent Assay (ELISA)

Fecal, serum, and hippocampal samples from mice were collected and subsequently stored at -80°C for analysis. The levels of TMAO, high-density lipoprotein (HDL), low-density lipoprotein (LDL), triglycerides (TG), and total cholesterol (TC) were quantified using ELISA kits from Jiangsu Meimian Industrial Co., Ltd. Following the manufacturer's guidelines, the samples were diluted and then added to ELISA plates that were pre-coated with specific antibodies. After incubation at room temperature in the dark, the plates were washed to remove unbound substances. Color development was then initiated and terminated using a stop solution. The absorbance was immediately measured at 450 nm, and sample concentrations were calculated using a standard curve. Each sample was assayed in duplicate.

Statistical Analysis

Statistical analyses were performed using SPSS software (version 26.0), whereas GraphPad Prism (version 9.0) was used for data visualization. Continuous data were assessed for normality using the Shapiro–Wilk test and for homogeneity of variance using Levene's test. For normally distributed data with equal variances, one-way analysis of variance was performed, followed by post hoc pairwise comparisons using the least significant difference test. Results are reported as the mean \pm standard deviation. For non-normally distributed data, the Kruskal–Wallis test was used, and results are presented as the median (interquartile range). All tests were two-tailed, and a P value < 0.05 was considered statistically significant.

Results

Antibiotic Disruption of Gut Microbiota Composition in Mice

The effects of antibiotics on the composition and structure of gut microbiota were evaluated using 16S rRNA sequencing. Microbiota profiling using Illumina sequencing yielded 1,347,904 high-quality reads and 566,850,360 total bases from fecal samples, with an average sequence length of 420 base pairs (bp). Differences in α -diversity between ABX-treated and CON mice were observed. The Chao1 ($P < 0.05$) and Simpson indices decreased ($P < 0.05$), whereas the Shannon index increased ($P < 0.05$) (Figure 1A–C). β -diversity analysis of mouse gut microbiota community composition indicated distinct clustering between groups. Principal component analysis demonstrated non-overlapping clusters for the CON and ABX groups, indicating substantial differences in community composition between these groups (Figure 1D). PCoA further confirmed the substantial dissimilarities in species composition between the CON and ABX groups, as evidenced by the non-overlapping clusters (Figure 1E).

Antibiotic-Induced Gut Microbiota Disruption Elevates TMAO Levels

Analysis of the mouse gut microbiota at the family level indicated distinct compositional differences between the CON and ABX groups. In the CON group, *Lactobacillaceae* was the most abundant family, whereas the ABX group exhibited higher abundances of *Lachnospiraceae*, *Bacteroidaceae*, and *Tannerellaceae* (Figure 2A–C). To investigate the overall changes in gut microbiota composition between the two groups, LEfSe was used to identify the key taxa driving the observed differences in fecal microbiota composition. The CON group was characterized by predominant taxa such as *Lactobacillales*, *Lactobacillaceae*, and *Lactobacillus*, as well as *Bacteroides* and *Prevotellaceae* (Figure 2D). Conversely, the ABX group exhibited dominant taxa including *Bacteroidia*, *Bacteroidales*, *Bacteroidaceae*, *Bacteroides*, *Gammaproteobacteria*, *Pseudomonadales*, *Pseudomonadaceae*, *Pseudomonas*, *Alcaligenes*, *Enterobacteriales*, *Morganellaceae*, and *Providencia*, with nearly depleted levels of *Lactobacillales*, *Lactobacillaceae*, and *Lactobacillus* (Figure 2E). qPCR validation of representative taxa was consistent with the 16S rRNA sequencing results. The relative abundance of *Lactobacillus* was significantly lower in the ABX and ABX+CIRI groups compared with the CON group (mean \pm SD: CON, 0.82 ± 0.11 ; ABX, 0.12 ± 0.03 ; CIRI, 0.75 ± 0.09 ; ABX+CIRI, 0.09 ± 0.02 ; $P < 0.001$ for ABX vs. CON and ABX+CIRI vs. CON). Conversely, the abundance of *Bacteroides* was markedly increased in the ABX and ABX+CIRI groups relative to the CON group (CON, 0.08 ± 0.02 ; ABX, 0.45 ± 0.07 ; CIRI, 0.11 ± 0.03 ; ABX+CIRI, 0.52 ± 0.08 ; $P < 0.001$) (Figure 2F).

To explore the potential mechanisms by which antibiotic-induced dysbiosis aggravates CIRI-related cognitive dysfunction, functional predictive analysis of the altered gut microbiota was performed. COG functional analysis indicated substantial differences in RNA processing and modification, cell cycle regulation, cell division, chromosome

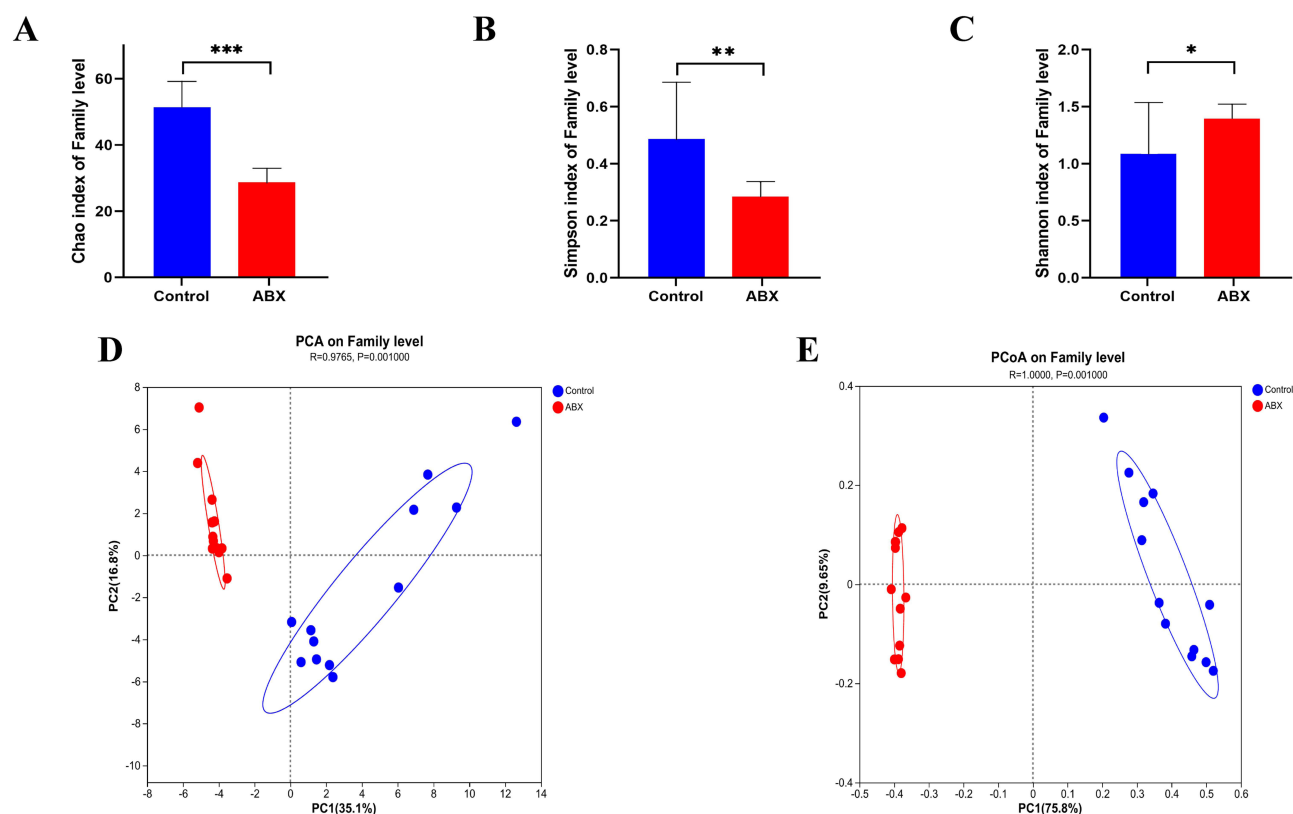


Figure 1 Antibiotic-induced gut microbiota composition disruption in mice. **(A)** Chao I index of the gut microbiota at the family level, showing a significant decrease in the ABX group compared with the Control group ($P < 0.001$). **(B)** Simpson index of the gut microbiota at the family level, showing a significant decrease in the ABX group compared with the Control group ($P = 0.002743$). **(C)** Shannon index of the gut microbiota at the family level, showing a significant increase in the ABX group compared with the Control group ($P = 0.03285$). **(D)** Principal component analysis (PCA) of gut microbiota composition. Closer distances in the PCA plot indicate greater similarity in species composition between samples. **(E)** Principal coordinate analysis (PCoA) of gut microbiota composition. Data are presented as mean \pm standard deviation (SD). * $P < 0.05$; ** $P < 0.01$; *** $P < 0.001$.

partitioning, lipid transport, and metabolism within the gut microbiota (Figure 3A). KEGG pathway analysis indicated enhanced amino acid and carbon metabolism with reduced fatty acid metabolism and synthesis in the intestinal microbiota of ABX-treated mice (Figure 3B). The gut microbiota database gutMGen²² identified genera such as Bacteroides and Escherichia that are associated with choline metabolism, TMAO production, and activation of inflammatory pathways (Figure 3D). ELISA measurements showed that TMAO concentrations were increased in the ABX + CIRI group compared with those of the CIRI group ($P < 0.05$) (Figure 3C). Given the close association between TMAO and lipid metabolism, elevated TMAO levels may represent a potential mechanism underlying CIRI-related cognitive dysfunction.

Gut Microbiota Dysbiosis Aggravates CIRI-Induced Cognitive Impairment

The MWM test was used to evaluate the spatial learning and memory capabilities of each mouse group. The total swimming distance was similar among the groups during both the navigation and probe trials ($P > 0.05$), suggesting that locomotor activity was not a major confounder. Over 4 days, all groups showed a progressive decrease in escape latency in the water maze spatial navigation test, indicating successful task acquisition (Figure 4A). Compared with the CON group, both the CIRI and ABX + CIRI groups showed prolonged escape latency, indicating impaired learning and memory following CIRI. The ABX + CIRI group experienced a longer escape latency than that of the CIRI group ($P < 0.05$), indicating more severe memory and cognitive deficits (Figure 4B).

In the water maze spatial probe test, both the CIRI and ABX + CIRI groups exhibited fewer platform crossings and reduced time spent in the target quadrant compared with those of the CON group ($P < 0.05$). The ABX + CIRI group showed fewer platform crossings and less time spent in the target area than that of the CIRI group ($P < 0.05$), indicating

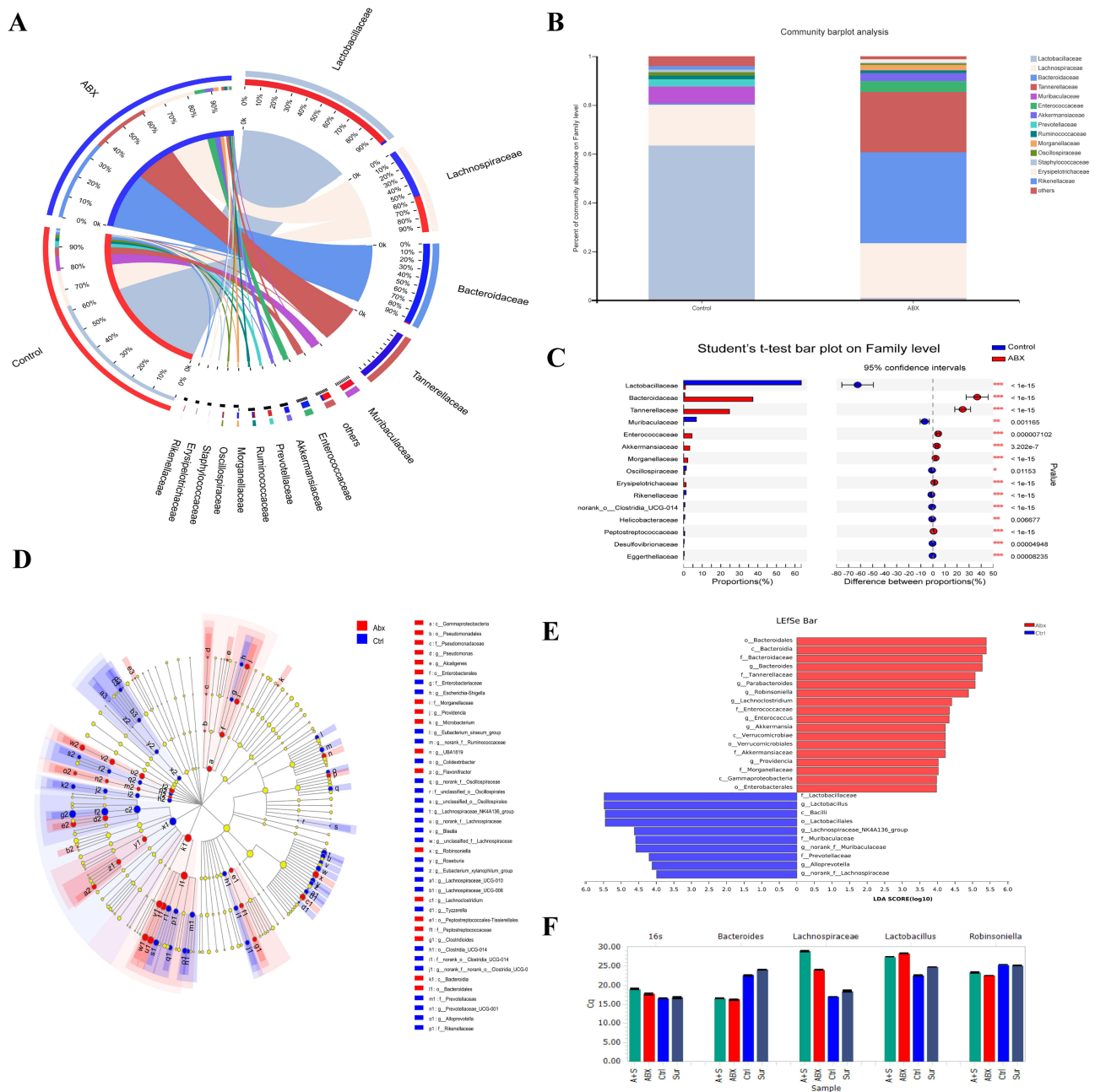


Figure 2 Effects of antibiotic therapy on the gut microbiome in mice. **(A)** Relationship diagram between samples and species. Outer-colored bands represent different groups, whereas inner bands denote species colored by their relative abundance in corresponding samples. **(B)** Mean relative abundance of gut microbiota at the family level in fecal samples from two mouse groups. **(C)** Comparative analysis of the dominant gut microbial taxa at the family level between the two mouse groups. **(D)** Bacterial taxa with substantial abundance differences between the two gut microbiota groups. The nodes represented in various colors illustrate microbial taxa that are substantially enriched in their respective groups and play a crucial role in the differences observed between groups. Nodes in pale yellow denote microbial taxa that do not show substantial differences between the groups or have minimal influence on the inter-group variations. **(E)** Linear discriminant analysis (LDA) bar plot. Elevated LDA scores reflect a greater influence of species abundance on differentiation effects. **(F)** Quantitative polymerase chain reaction validation of representative taxa. Data are presented as mean ± standard deviation (SD). A + (C) ABX + CIRI; ABX, antibiotics; CIRI, cerebral ischemia–reperfusion injury.

worse performance and further impairment of memory and cognitive function compared with that of the CIRI group (Figure 4C–E). The MWM experiments suggest that both ABX and CIRI contribute to cognitive impairment in mice, with ABX exacerbating the cognitive deficits induced by CIRI.

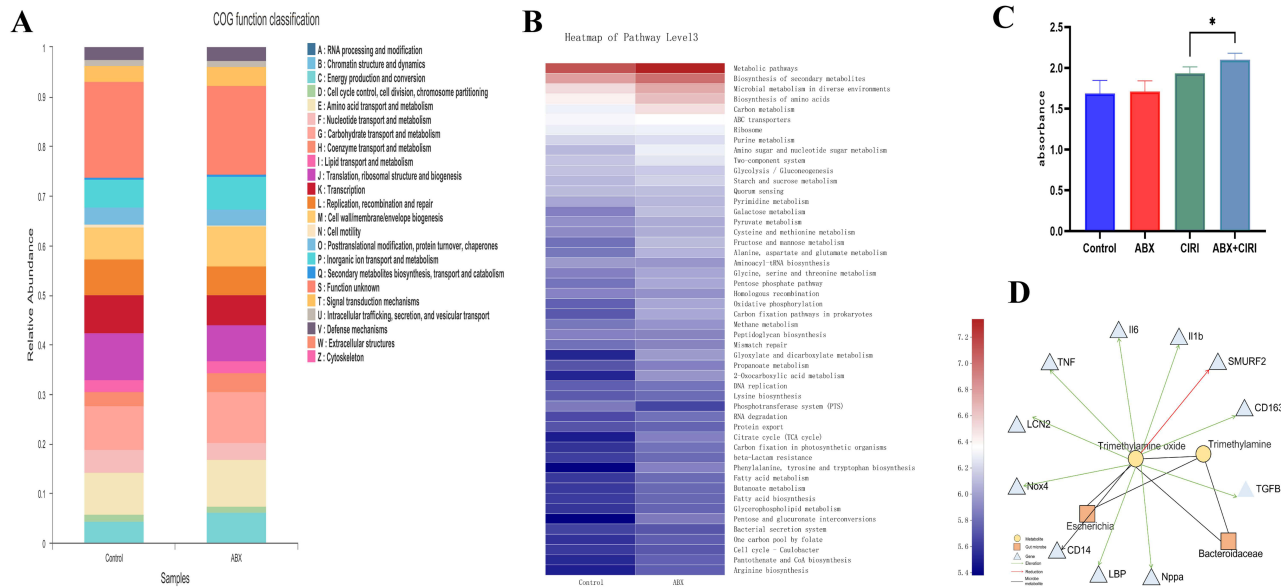


Figure 3 Metabolic disruption and increased trimethylamine N-oxide (TMAO) caused by antibiotic use in mice. **(A)** Enrichment of Clusters of Orthologous Groups (COG) functional categories in the two groups of mice. **(B)** Enrichment of Kyoto Encyclopedia of Genes and Genomes (KEGG) functional pathways in the two groups of mice. **(C)** Serum TMAO levels in mice. TMAO concentration is substantially higher in the antibiotic treatment (ABX) + cerebral ischemia-reperfusion injury (CIRI) group compared with that in the CIRI group ($P = 0.0375$). **(D)** Interaction diagram between differential gut microbiota, genes, and metabolic products. Green and red arrows indicate gene activation and inhibition, respectively. Black lines represent connections with gut microbiota metabolites. Data are presented as mean \pm standard deviation (SD).

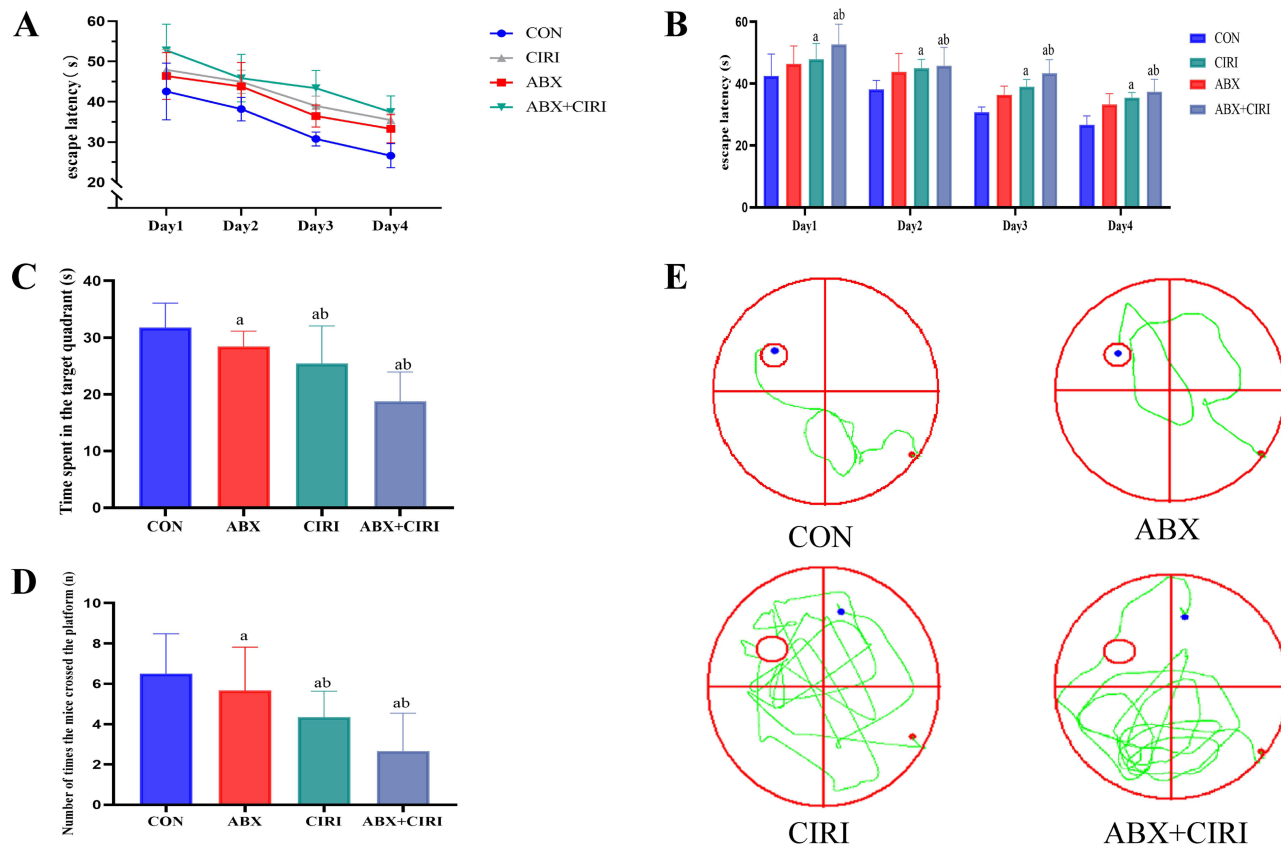


Figure 4 Gut microbiota disruption aggravates cerebral ischemia-reperfusion injury (CIRI)-induced cognitive impairment. **(A)** Line graph showing escape latency in the Morris water maze (MWM) test for each group of mice. **(B)** Bar graph illustrating escape latency in the MWM test for each group of mice. **(C)** Bar graph depicting time spent in the target quadrant during the spatial exploration trial of the MWM test for each group of mice. **(D)** Bar graph displaying the number of platform crossings during the spatial exploration trial of the MWM test for each group of mice. **(E)** Representative movement trajectories of mice during the spatial exploration trial of the MWM test for each group. Data are presented as mean \pm standard deviation (SD). ^a $P < 0.01$ vs. CON group; ^b $P < 0.05$ vs. CIRI group.

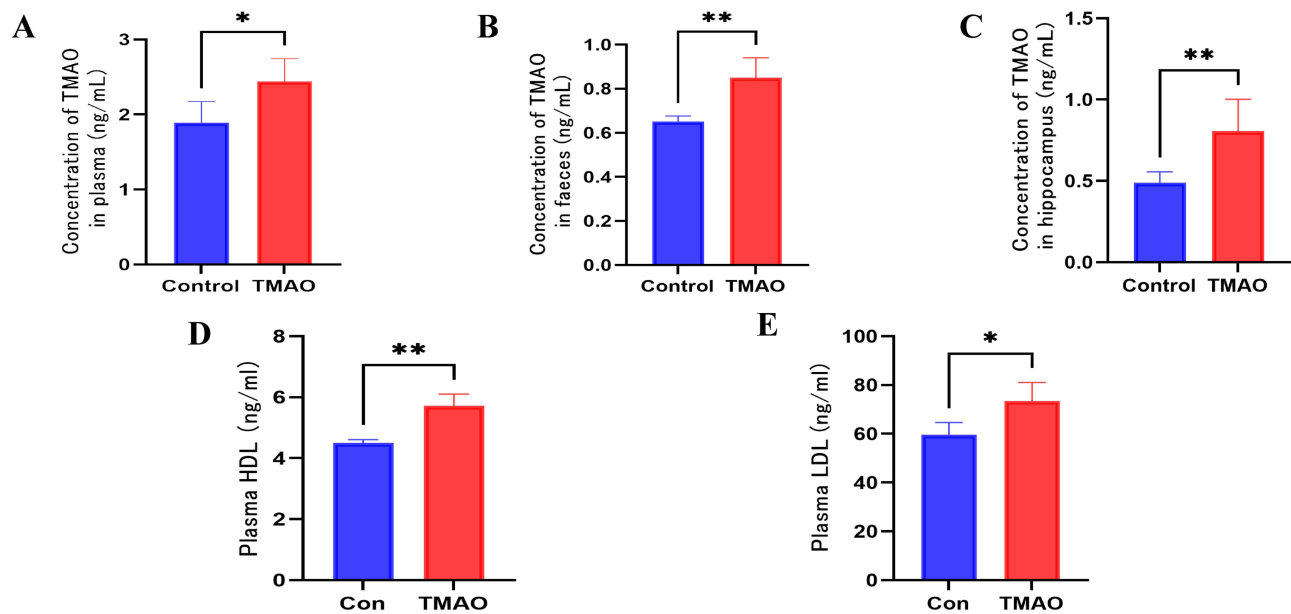


Figure 5 Intraperitoneal injection of trimethylamine N-oxide (TMAO) elevates TMAO levels in feces, serum, and the hippocampus, impacting lipid metabolism. (A) Intraperitoneal injection of TMAO increases serum TMAO levels in mice ($P = 0.0174$). (B) Intraperitoneal injection of TMAO increases fecal TMAO levels in mice ($P = 0.0068$). (C) Intraperitoneal injection of TMAO increases hippocampal TMAO levels in mice ($P = 0.0088$). (D) Intraperitoneal injection of TMAO increases serum high-density lipoprotein (HDL) levels in mice ($P = 0.0036$). (E) Intraperitoneal injection of TMAO increases serum low-density lipoprotein (LDL) levels in mice ($P = 0.0254$). Data are presented as mean \pm standard deviation (SD); * $P < 0.05$; ** $P < 0.01$.

TMAO Upregulation Aggravates CIRI-Induced Cognitive Impairment

To confirm the role of TMAO in exacerbating cognitive impairment induced by gut microbiota disruption in CIRI, mice were intraperitoneally injected with TMAO. Levels of the intestinal-derived metabolite TMAO in mouse plasma, feces, and hippocampus were assessed using ELISA to confirm successful elevation *in vivo*. Compared with the CON group, increases in TMAO concentrations were observed in the plasma ($P < 0.05$), feces ($P < 0.01$), and hippocampus ($P < 0.01$) of the TMAO group (Figure 5A–C). ELISA indicated that, relative to the CON group, levels of HDL ($P < 0.01$) and LDL ($P < 0.05$) were elevated in the TMAO group, whereas no marked differences were noted in TG and TC levels (Figure 5D and E).

Learning and memory function in CIRI mice, with and without TMAO upregulation, was evaluated using the MWM. In the place navigation test, the escape latency progressively decreased over 4 days in all groups, suggesting successful task acquisition (Figure 6A). During the spatial probe test, both the CIRI and TMAO + CIRI groups exhibited fewer platform crossings and reduced time spent in the target quadrant compared with those of the CON group ($P < 0.05$). The TMAO + CIRI group demonstrated substantially fewer platform crossings and spent less time in the target quadrant than those of the CIRI group ($P < 0.05$), indicating more severe impairments in memory and cognitive function (Figure 6B–D).

Overall, these findings suggest that TMAO upregulation may exacerbate CIRI-associated cognitive impairment, although the observed lipid-related changes are exploratory and require further validation. The total swimming distance did not differ significantly among groups during either the navigation or probe trials ($P > 0.05$), indicating that the observed cognitive differences were not attributable to locomotor deficits.

Discussion

Administration of a combination of ciprofloxacin, ampicillin, streptomycin, and clindamycin induced gut microbiota dysbiosis in mice and exacerbated CIRI-related cognitive impairment, an effect associated with elevated TMAO levels.

The gut microbiome constitutes a complex microbial system in the gastrointestinal tract and is involved in various metabolic pathways, signal transduction, and modulation of the immune-inflammatory axis.²³ Antibiotics, as a primary intervention, alter the gut microbiota, disrupt microbial homeostasis, and affect cognitive function. Mice treated with ampicillin alone exhibited a reduction in Firmicutes abundance, leading to spatial memory deficits in the MWM test and

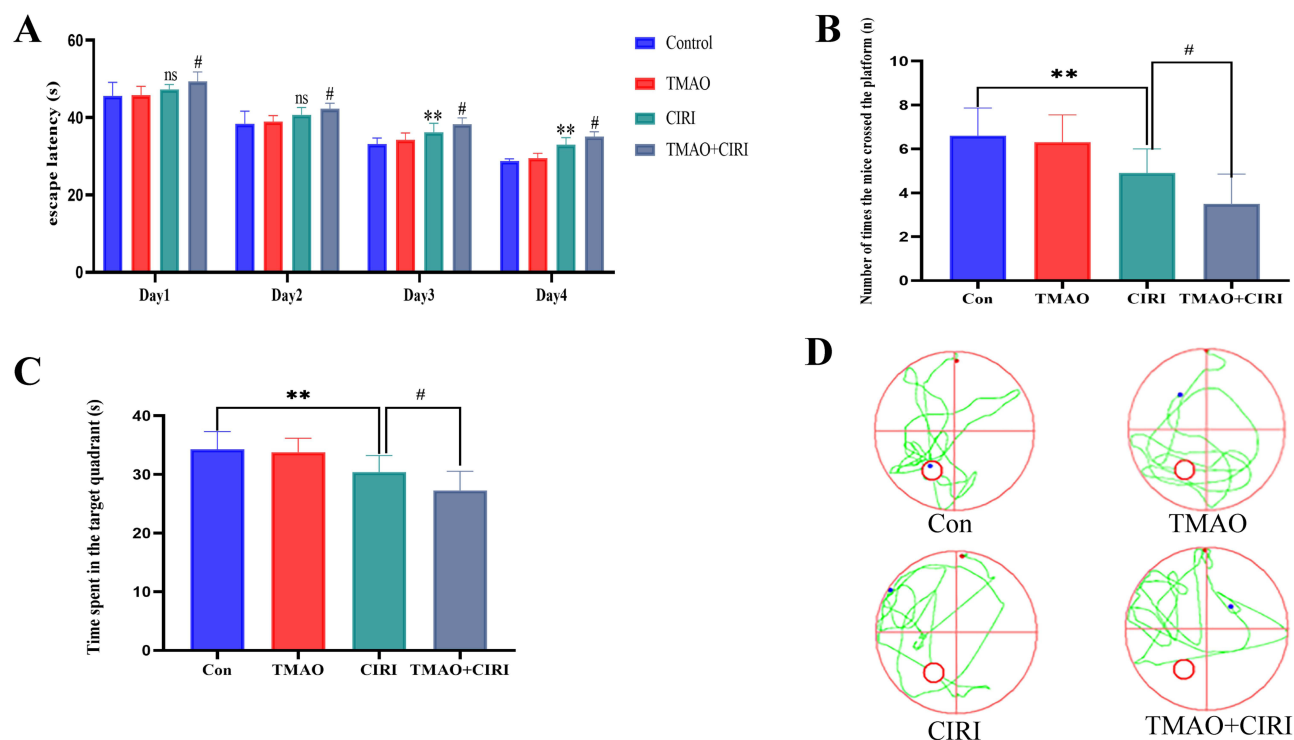


Figure 6 Trimethylamine N-oxide (TMAO) exacerbates cerebral ischemia–reperfusion injury (CIRI)-induced cognitive impairment. **(A)** Bar graph showing escape latency in the Morris water maze (MWM) place navigation test for each group of mice. **(B)** Number of platform crossings in the MWM spatial probe test for each group of mice. **(C)** Time spent in the target area in the MWM spatial probe test for each group of mice. **(D)** Movement trajectories in the MWM spatial probe test for each group of mice. Data are presented as mean \pm standard deviation (SD); ns: not significant vs. Control group; **P < 0.01 vs. Control group; #P < 0.05 vs. CIRI group.

impaired novel object recognition memory.²⁴ Similarly, a combination of ciprofloxacin and metronidazole substantially affected the richness and diversity of the gut microbiota, restructuring microbial composition and exacerbating working memory impairment in mice.²⁵ Lincomycin treatment reduces the relative abundance of Firmicutes and increases the abundance of Bacteroidetes in mice, accompanied by decreased cognitive flexibility.²⁶ Behavioral studies in mice treated with clindamycin also indicate reduced recognition memory and increased signs of depression.²⁷ Treatment with vancomycin and ampicillin in mice with transient forebrain ischemia increased the abundance of Proteobacteria and worsened cognitive impairment in tasks, such as the Y-maze, novel object recognition, and Barnes maze.²⁸ Combination therapies, such as ampicillin, vancomycin, metronidazole, and imipenem, non-selectively deplete the intestinal microbiota, resulting in reduced microbial abundance and bacterial diversity, leading to impaired novel object recognition memory in mice.²⁹

Collectively, these studies suggest that short-term treatment with a single antibiotic or antibiotic combinations disrupts the gut microbiota and impairs cognitive function. The present study, which used a combination of ciprofloxacin, ampicillin, streptomycin, and clindamycin in mice, supports previous findings.

Using 16S rDNA sequencing, antibiotic treatment was shown to disrupt gut microbiota diversity, leading to reduced levels of *Lactobacillus* in mice. In contrast, the peri-operative administration of cefazolin was found to reverse anesthesia- and surgery-induced dysbiosis, mitigate cognitive impairment related to these procedures, enhance blood–brain barrier integrity, and increase the expression of tight junction proteins; cefazolin may exert different effects compared to the other antibiotics studied.³⁰

Treatment of mice with an antibiotic cocktail did not induce cognitive impairment. However, antibiotic pretreatment exacerbated cognitive deficits following CIRI. Prior to CIRI, these mice showed an increased abundance of Proteobacteria and *Tannerellaceae*, along with a reduction in *Lactobacillus*. A study analyzing fecal samples from healthy controls and patients with AD found distinct differences in gut microbiota richness between the two groups. Individuals with AD exhibited higher abundances of Bacteroidetes and Proteobacteria, with reduced levels of Firmicutes and Actinobacteria at the phylum level. At the family level, *Clostridiaceae*, *Streptococcaceae*, and *Bifidobacteriaceae* were decreased, whereas *Enterobacteriaceae* and *Erysipelotrichaceae* were increased.³¹ The 16S rRNA gene sequencing in patients with depression and cognitive impairment

showed a decrease in the abundance of Firmicutes at the phylum level and an increase in Bacteroidetes, Actinobacteria, and Proteobacteria. At the family level, there was a decrease in *Clostridiaceae* and *Streptococcaceae* and an increase in *Helicobacteraceae*.³² A reduction in *Clostridiaceae* has been associated with exacerbated cognitive impairment, with evidence suggesting causal links between gut microbiota, metabolites, and cognitive performance.² Thus, alterations in the gut microbiota and metabolites may increase the risk of CIRI-induced cognitive impairment.

Alterations in metabolites derived from gut microbiota occur due to dysbiosis and impact cognitive function. Using a microbial metabolite database, antibiotic treatment was predicted to increase TMAO levels. ELISA subsequently confirmed elevated TMAO concentrations following gut microbiota dysbiosis. Trimethylamine (TMA) is a derivative of dietary choline and carnitine produced by various gut microbiota.³³ TMA enters the systemic circulation through the hepatic portal system after being absorbed by the portal circulation. TMA then travels to the liver, where flavin-containing monooxygenases convert it into TMAO.³⁴ TMAO may exacerbate vascular inflammation, increase reactive oxygen species production, and increase the risk of atherosclerosis.³⁵ TMAO can cross the blood–brain barrier and induce inflammatory responses and neural damage in the brain. In cerebral ischemia models, TMAO activates microglial inflammasomes.¹⁸ Beyond our observations, TMAO has been reported to impair gut-brain integrity and induce synaptic dysfunction, as well as to exacerbate neuroinflammation and microglial activation, mechanisms that may collectively contribute to cognitive deficits after CIRI.³⁶ TMAO administration substantially elevates its levels in both plasma and cerebrospinal fluid, promoting oligodendrocyte pyroptosis and demyelination via oxidative stress and NLRP3 pathway activation.³⁷ This provides experimental evidence for the present study.

The present findings indicate that increasing TMAO levels via intraperitoneal injection mimics antibiotic-induced gut microbiota dysbiosis and exacerbates CIRI-induced cognitive impairment. A study involving transplantation of human gut microbiota with low and high TMAO-producing capacity into germ-free mice demonstrated that TMAO levels directly influenced infarct size and adverse post-stroke outcomes.³⁸ Zhao et al also observed that elevated TMAO levels suppressed hippocampal glutathione reductase A expression induced by sevoflurane in older rats, increased brain sensitivity to oxidative stress, activated hippocampal microglia, and enhanced the release of proinflammatory factors, ultimately aggravating sevoflurane-induced cognitive impairment in older rats.³⁹ Therefore, TMAO, a gut microbiota–derived metabolite, is intrinsically linked to central nervous system disorders and is associated with cognitive dysfunction as well as vascular diseases.

KEGG pathway analysis indicated that the fatty acid metabolism and synthesis pathways were downregulated in the ABX group, whereas TMAO was also associated with lipid metabolism. Consistent with our findings on TMAO-mediated lipid alterations, Zhang et al recently demonstrated that modulation of lipid metabolism alleviates post-stroke cognitive impairment in cerebral ischemia/reperfusion rats, further supporting the relevance of lipid-related pathways in this setting.⁴⁰ Therefore, lipid-related indicators were further assessed for validation. The LDL levels in the TMAO group were substantially higher than those in the CON group. A study on middle-aged and older individuals found that cognitive impairment and depression were associated with high HDL levels.⁴¹ Patients with dyslipidemia were more likely to experience cognitive impairment than those with normal blood lipid levels.⁴² The observed changes in HDL and LDL suggest a possible association; however, the relationship between TMAO, lipid metabolism, and cognitive impairment was not directly tested in this study and should therefore be interpreted with caution. Larger studies will be needed to confirm these findings. These findings also suggest that interventions aimed at reducing TMAO production, such as dietary modification or microbiota-targeted strategies, may warrant further investigation.

This study has some limitations. Only male mice were used; therefore, sex-specific differences in gut microbiota composition and stroke outcomes were not assessed. We did not monitor daily water consumption during antibiotic treatment; therefore, potential differences in antibiotic intake due to altered drinking behavior cannot be completely excluded. We did not monitor body weight or adjust the TMAO dose accordingly. Although the fixed dose was based on published protocols, potential effects of body weight variability on TMAO exposure cannot be ruled out. The TMAO validation cohort was small, and the lipid-related findings were exploratory. In addition, the downstream molecular mechanisms by which TMAO aggravates CIRI-induced cognitive impairment were not directly tested. Future studies should consider fecal microbiota transplantation, mechanistic validation, and sex-based comparisons.

Conclusion

Antibiotic-induced gut dysbiosis aggravates CIRI-related cognitive impairment and is associated with increased TMAO levels. These findings support a potential gut microbiota–metabolite axis in post-ischemic cognitive dysfunction.

Data Sharing Statement

The original contributions presented in the study are publicly available. This data can be found here: <https://www.ncbi.nlm.nih.gov/sra/PRJNA1299159>. Further inquiries can be directed to the corresponding author.

Ethics Statement

This study was approved by the Animal Ethics Committee of Southwest Medical University (Approval number: swmu20220073). This study was conducted in strict accordance with the National Institutes of Health Guide for the Care and Use of Laboratory Animals (8th edition, 2011), and reporting followed the ARRIVE guidelines for animal research.

Author Contributions

All authors made a significant contribution to the work reported, whether that is in the conception, study design, execution, acquisition of data, analysis and interpretation, or in all these areas; took part in drafting, revising or critically reviewing the article; gave final approval of the version to be published; have agreed on the journal to which the article has been submitted; and agree to be accountable for all aspects of the work.

Funding

This work was supported by the Campus-institute Strategic Cooperation Project (grant number 2024SNXNYD01); Campus-institute strategic cooperation projects of Southwest Medical University(2025HJXNYD05).

Disclosure

The authors declare that the research was conducted in the absence of any commercial or financial relationships that could be construed as a potential conflict of interest.

References

1. Aben HP, De Munter L, Reijmer YD, et al. Prediction of cognitive recovery after stroke: the value of diffusion-weighted imaging–based measures of brain connectivity. *Stroke*. 2021;52(6):1983–1992. doi:10.1161/STROKEAHA.120.032033
2. Cao W, Xing M, Liang S, Shi Y, Li Z, Zou W. Causal relationship of gut microbiota and metabolites on cognitive performance: a mendelian randomization analysis. *Neurobiol Dis*. 2024;191:106395. doi:10.1016/j.nbd.2023.106395
3. Zhang X, Huang Y, Han X, Wang Y, Zhang L, Chen L. Evaluating the protective effects of mitochondrial glutathione on cerebral ischemia/reperfusion injury via near-infrared fluorescence imaging. *Anal Chem*. 2019;91(22):14728–14736. doi:10.1021/acs.analchem.9b04082
4. Zhao Z, Lu C, Li T, et al. The protective effect of melatonin on brain ischemia and reperfusion in rats and humans: in vivo assessment and a randomized controlled trial. *J Pineal Res*. 2018;65(4):e12521. doi:10.1111/jpi.12521
5. Graber M, Garnier L, Mohr S, et al. Influence of pre-existing mild cognitive impairment and dementia on post-stroke mortality. The Dijon Stroke Registry. *Neuroepidemiology*. 2020;54(6):490–497. doi:10.1159/000497614
6. Cui G, Li S, Ye H, et al. Gut microbiome and frailty: insight from genetic correlation and mendelian randomization. *Gut Microbes*. 2023;15(2):2282795. doi:10.1080/19490976.2023.2282795
7. Singh RK, Chang H-W, Yan D, et al. Influence of diet on the gut microbiome and implications for human health. *J Transl Med*. 2017;15:1–17. doi:10.1186/s12967-017-1175-y
8. Dohm-Hansen S, Donoso F, Lucassen PJ, Clarke G, Nolan YM. The gut microbiome and adult hippocampal neurogenesis: a new focal point for epilepsy? *Neurobiol Dis*. 2022;170:105746. doi:10.1016/j.nbd.2022.105746
9. Cryan JF, O’Riordan KJ, Sandhu K, Peterson V, Dinan TG. The gut microbiome in neurological disorders. *Lancet Neurol*. 2020;19(2):179–194. doi:10.1016/S1474-4422(19)30356-4
10. Xia G-H, You C, Gao -X-X, et al. Stroke dysbiosis index (SDI) in gut microbiome are associated with brain injury and prognosis of stroke. *Front Neurol*. 2019;10:397. doi:10.3389/fneur.2019.00397
11. Wang H, Zhang M, Li J, et al. Gut microbiota is causally associated with poststroke cognitive impairment through lipopolysaccharide and butyrate. *J Neuroinflammation*. 2022;19(1):76. doi:10.1186/s12974-022-02435-9
12. Chen C, Liao J, Xia Y, et al. Gut microbiota regulate Alzheimer’s disease pathologies and cognitive disorders via PUFA-associated neuroinflammation. *Gut*. 2022;71(11):2233–2252. doi:10.1136/gutjnl-2021-326269
13. Osadchiy V, Martin CR, Mayer EA. The gut–brain axis and the microbiome: mechanisms and clinical implications. *Clin Gastroenterol Hepatol*. 2019;17(2):322–332. doi:10.1016/j.cgh.2018.10.002

14. Grabrucker S, Marizzoni M, Silajdžić E, et al. Microbiota from Alzheimer's patients induce deficits in cognition and hippocampal neurogenesis. *Brain*. 2023;146(12):4916–4934. doi:10.1093/brain/awad303
15. Sherwin E, Dinan TG, Cryan JF. Recent developments in understanding the role of the gut microbiota in brain health and disease. *Ann N Y Acad Sci*. 2018;1420(1):5–25. doi:10.1111/nyas.13416
16. Fiaschini N, Mancuso M, Tanori M, et al. Liver steatosis and steatohepatitis alter bile acid receptors in brain and induce neuroinflammation: a contribution of circulating bile acids and blood-brain Barrier. *Int J Mol Sci*. 2022;23(22):14254. doi:10.3390/ijms232214254
17. Enko D, Zelzer S, Niedrist T, et al. Assessment of trimethylamine-N-oxide at the blood-cerebrospinal fluid barrier: results from 290 lumbar punctures. *EXCLI J*. 2020;19:1275. doi:10.17179/excli2020-2763
18. Ji X, Tian L, Niu S, Yao S, Qu C. Trimethylamine N-oxide promotes demyelination in spontaneous hypertension rats through enhancing pyroptosis of oligodendrocytes. *Front Aging Neurosci*. 2022;14:963876. doi:10.3389/fnagi.2022.963876
19. Tirelle P, Breton J, Riou G, Déchelotte P, Coëffier M, Ribet D. Comparison of different modes of antibiotic delivery on gut microbiota depletion efficiency and body composition in mouse. *BMC Microbiol*. 2020;20(1):340. doi:10.1186/s12866-020-02018-9
20. Hong S, Lu J, Li J, et al. Protective role of (-)-epicatechin on trimethylamine-N-oxide (TMAO)-induced cardiac hypertrophy via SP1/SIRT1/SUMO1 signaling pathway. *Cardiovasc Toxicol*. 2024;24(12):1335–1347. doi:10.1007/s12012-024-09932-8
21. Wang P, Mi Y, Yu H, et al. Trimethylamine-N-oxide aggravated the sympathetic excitation in D-galactose induced aging rats by down-regulating P2Y12 receptor in microglia. *Biomed Pharmacother*. 2024;174:116549. doi:10.1016/j.biopha.2024.116549
22. Cheng L, Qi C, Yang H, et al. gutMGene: a comprehensive database for target genes of gut microbes and microbial metabolites. *Nucleic Acids Res*. 2022;50(D1):D795–D800. doi:10.1093/nar/gkab786
23. Ferreira AL, Choi J, Ryou J, et al. Gut microbiome composition may be an indicator of preclinical Alzheimer's disease. *Sci Transl Med*. 2023;15(700):eabo2984. doi:10.1126/scitranslmed.abo2984
24. Sarkar SR, Mazumder PM, Chatterjee K, et al. *Saccharomyces boulardii* ameliorates gut dysbiosis associated cognitive decline. *Physiol Behav*. 2021;236:113411. doi:10.1016/j.physbeh.2021.113411
25. Zhao Z, Cui D, Wu G, et al. Disrupted gut microbiota aggravates working memory dysfunction induced by high-altitude exposure in mice. *Front Microbiol*. 2022;13:1054504. doi:10.3389/fmicb.2022.1054504
26. Tamada H, Ikuta K, Makino Y, et al. Impact of intestinal microbiota on cognitive flexibility by a novel touch screen operant system task in mice. *Front Neurosci*. 2022;16:882339. doi:10.3389/fnins.2022.882339
27. Kwon H-J, Mohammed AE, Eltom KH, Albrahim JS, Alburay NA. Evaluation of antibiotic-induced behavioral changes in mice. *Physiol Behav*. 2020;223:113015. doi:10.1016/j.physbeh.2020.113015
28. Lee K-E, Kim J-K, Kim D-H. Orally administered antibiotics vancomycin and ampicillin cause cognitive impairment with gut dysbiosis in mice with transient global forebrain ischemia. *Front Microbiol*. 2020;11:564271. doi:10.3389/fmicb.2020.564271
29. Fröhlich EE, Farzi A, Mayerhofer R, et al. Cognitive impairment by antibiotic-induced gut dysbiosis: analysis of gut microbiota-brain communication. *Brain Behav Immun*. 2016;56:140–155. doi:10.1016/j.bbi.2016.02.020
30. Luo A, Li S, Wang X, Xie Z, Li S, Hua D. Cefazolin improves anesthesia and surgery-induced cognitive impairments by modulating blood-brain barrier function, gut bacteria and short chain fatty acids. *Front Aging Neurosci*. 2021;13:748637. doi:10.3389/fnagi.2021.748637
31. D'Argenio V, Veneruso I, Gong C, Cecarini V, Bonfili L, Eleuteri AM. Gut microbiome and Mycobiome alterations in an in vivo model of Alzheimer's disease. *Genes*. 2022;13(9):1564. doi:10.3390/genes13091564
32. Liu L, Wang H, Chen X, Zhang Y, Zhang H, Xie P. Gut microbiota and its metabolites in depression: from pathogenesis to treatment. *EBioMedicine*. 2023;90:104527. doi:10.1016/j.ebiom.2023.104527
33. Wang Z, Bergeron N, Levison BS, et al. Impact of chronic dietary red meat, white meat, or non-meat protein on trimethylamine N-oxide metabolism and renal excretion in healthy men and women. *Eur Heart J*. 2019;40(7):583–594. doi:10.1093/eurheartj/ehy799
34. Saadoud F, Liu L, Xu K, et al. Aorta-and liver-generated TMAO enhances trained immunity for increased inflammation via ER stress/mitochondrial ROS/glycolysis pathways. *JCI Insight*. 2023;8(1). doi:10.1172/jci.insight.158183
35. Ma S-R, Tong Q, Lin Y, et al. Berberine treats atherosclerosis via a vitamine-like effect down-regulating Choline-TMA-TMAO production pathway in gut microbiota. *Signal Transduct Target Ther*. 2022;7(1):207. doi:10.1038/s41392-022-01027-6
36. Su M, Tang T, Tang W, Long Y, Wang L, Liu M. Astragalus improves intestinal barrier function and immunity by acting on intestinal microbiota to treat T2DM: a research review. Review. *Front Immunol*. 2023;14. doi:10.3389/fimmu.2023.1243834
37. Zhang Y, Wang G, Li R, et al. Trimethylamine N-oxide aggravated cognitive impairment from APP/PS1 mice and protective roles of voluntary exercise. *Neurochem Int*. 2023;162:105459. doi:10.1016/j.neuint.2022.105459
38. Zhu W, Romano KA, Li L, et al. Gut microbes impact stroke severity via the trimethylamine N-oxide pathway. *Cell Host Microbe*. 2021;29(7):1199–1208.e5. doi:10.1016/j.chom.2021.05.002
39. Momeni M, Khalifa C, Lemaire G, et al. Propofol plus low-dose dexmedetomidine infusion and postoperative delirium in older patients undergoing cardiac surgery. *Br J Anaesth*. 2021;126(3):665–673. doi:10.1016/j.bja.2020.10.041
40. Zhang H, Wang L, Wang X, et al. Mangiferin alleviated poststroke cognitive impairment by modulating lipid metabolism in cerebral ischemia/reperfusion rats. *Eur J Pharmacol*. 2024;977:176724. doi:10.1016/j.ejphar.2024.176724
41. Liu YH, Chen MT, He YY, et al. Cognitive impairment and depression precede increased HDL-C levels in middle-aged and older Chinese adults: cross-lagged panel analyses. *Lipids Health Dis*. 2024;23(1):288. doi:10.1186/s12944-024-02285-9
42. Zhao Y, Zhong K, Zheng Y, et al. Postoperative delirium risk in patients with hyperlipidemia: a prospective cohort study. *J Clin Anesth*. 2024;98:111573. doi:10.1016/j.jclinane.2024.111573

International Journal of General Medicine

Publish your work in this journal

The International Journal of General Medicine is an international, peer-reviewed open-access journal that focuses on general and internal medicine, pathogenesis, epidemiology, diagnosis, monitoring and treatment protocols. The journal is characterized by the rapid reporting of reviews, original research and clinical studies across all disease areas. The manuscript management system is completely online and includes a very quick and fair peer-review system, which is all easy to use. Visit <http://www.dovepress.com/testimonials.php> to read real quotes from published authors.

Submit your manuscript here: <https://www.dovepress.com/international-journal-of-general-medicine-journal>

Dovepress
Taylor & Francis Group